Acta Cryst. (1985). A**41**, 513-517

X-ray Diffraction Line Shapes from Bent Crystals with Linear Strain

BY SATISH RAO AND C. R. HOUSKA

Department of Materials Engineering, Virginia Polytechnic Institute and State University, Blacksburg, VA 24061, *USA*

(*Received* 1 *August* 1984; *accepted* 25 *April* 1985)

Abstract

This paper provides an exact solution for the X-ray diffraction line shape from a bent crystal with linear strain. Such crystals may be found along concentration gradients in a diffusion or ion-implanted zone, thin films and cold-worked materials. The solution simplifies into a sum of squares of two pairs of Fresnel integrals, which can be evaluated with very little computer time. The limiting cases of both pure particle-size broadening and pure strain broadening are also considered. Instrumental broadening is introduced by a numerical convolution with a Pearson VII function. A method of determining the linear strain and crystal size from experimental data is discussed.

Introduction

One can obtain the same general kinematic form for the X-ray diffraction line shape from two starting points. For example, Wilson (1949) treated the problem of diffraction from bent lamellae. Later, Houska (1970) described the d-spacing profile for a binary diffusion zone by a system of connecting elements with linearly incremented spacings. Each of these efforts was independent but arrives at very similar equations beginning from what appeared to be different initial problems. Houska (1970) began with a Fourier series for a linear change in d spacing and obtained the following result for a $00l$ reflection:

$$I(h_3) = N_3 \sum_{-(N_3-1)}^{(N_3-1)} C_n \exp(2\pi i n h_3)$$

$$C_n = \sin \pi[(\Delta d/\langle d\rangle)l]n[1-(|n|/N_3)]/\pi(\Delta d/\langle d\rangle)ln. \quad (1)$$

The various quantities are $h_3 = 2\langle d\rangle \sin\theta/\lambda$ with $\langle d\rangle$ determined from the θ_0 value at the midpoint of a first-order symmetrical intensity distribution ($h_3 = 1$) using X-rays of wavelength λ. Also, Δd represents the full change in d spacing between two extreme ends of a stack of N_3 atomic planes and n refers to nth-neighbor pairs of planes.

Equation (1) can also be written as an integral by making the substitutions

$$\mu = n/N_3, \quad s = (\Delta d/\langle d\rangle)lN_3 \quad \text{and} \quad h_3^0 = N_3(h_3 - l).$$

An integral form was used by Wilson (1949) and is given by

$$I(h_3^0)/2N_3^2 = \int_0^1 \frac{\sin \pi s\mu(1-\mu)}{\pi s\mu} \cos 2\pi\mu h_3^0 \, d\mu. \quad (2)$$

Wilson related s to the bending radius and elastic constants but did not give an explicit expression for the line shape. An examination of the line profile described by (1) requires a time-consuming synthesis of a Fourier series. Houska (1978) obtained an approximation for the line shape, which is based upon (2), that is valid only for small values of s.

The parameter s is related to the bending radius R by

$$s = (N_3^2\langle d\rangle/R)l|(q^2 - \nu p^2)/p|, \quad (2a)$$

where ν is Poisson's ratio, p and q are the direction cosines of the reflecting planes with respect to the x and y axes. Also, z is parallel to the reflection planes and the axis of bending, x is perpendicular to the bent lamella and y is perpendicular to x and z. Equations (1) and (2) are valid irrespective of whether the crystal is bent concave or convex.

From the experimental results of White (1950) using 500 μm quartz crystals and Mo radiation, it can be inferred that when the absolute value of the bending radius is less than 1 m or $\Delta d/\langle d\rangle$ is greater than 5×10^{-4} kinematic scattering theory is valid to better than 5%. For most measurements with a conventional diffractometer, one normally satisfies the conditions required for kinematic theory to be applicable.

If a double-crystal spectrometer is used, the overall sample broadening should be at least a factor of ten greater than the natural width of the undeformed crystal.

This paper provides an exact kinematic solution that simplifies into two pairs of Fresnel integrals, which was not given in the earlier work. The Fresnel integrals are approximated with an error $\leq 0{\cdot}2\%$ and require only a small number of well behaved terms that may be evaluated with very little computer time. Instrumental broadening is introduced by a numerical convolution with a Pearson VII function. An estimate of $\Delta d/\langle d\rangle$ (or bending radius) and N_3 can be made from the width of the diffraction peak and the number

0108-7673/85/060513-05$01.50

of major oscillations found within this region. It is possible to refine these estimates further by a least-squares fitting of the convoluted function with the experimental profiles.

Theory

Equation (2) may be written as

$$I(h_3^0)/2N_3^2 = -(2/s)\int_0^1\int_{h_3^0}\sin[\pi s\mu(1-\mu)] \times\sin 2\pi\mu h_3^0\,\mathrm{d}\mu\,\mathrm{d}h_3^0$$

or

$$I(h_3^0)/2N_3^2 = (1/s)\int_0^1\int_{h_3^0}\{\cos[\pi s\mu^2-2\pi(s/2+h_3^0)\mu] - \cos[\pi s\mu^2-2\pi(s/2-h_3^0)\mu]\}\,\mathrm{d}h_3^0\,\mathrm{d}\mu. \quad (3)$$

This is simplified by reversing the order of integration and making use of the tabulated integral (Abramowitz & Stegun, 1964)

$$\int\cos(ax^2+2bx+c)\,\mathrm{d}x = (\pi/2a)^{-1/2}\{\cos[(b^2-ac)a]C[(2/a\pi)^{1/2}(ax+b)] + \sin[(b^2-ac)/a]S[(2/a\pi)^{1/2}(ax+b)]\}.$$

The Fresnel functions are defined by

$$C(x)=\int_0^x\cos(\pi t^2/2)\,\mathrm{d}t$$

$$S(x)=\int_0^x\sin(\pi t^2/2)\,\mathrm{d}t$$

$$C(-x)=-C(x);\quad S(-x)=-S(x).$$

Combining terms and inserting limits, we get

$$\int_0^1\cos[\pi s\mu^2-2\pi(s/2+h_3^0)\mu]\,\mathrm{d}\mu = (2s)^{-1/2}(\cos[(\pi/s)(s/2+h_3^0)^2] \times\{C[(2/s)^{1/2}(s/2-h_3^0)] + C[(2/s)^{1/2}(s/2+h_3^0)]\} + \sin[(\pi/s)(s/2+h_3^0)^2] \times\{S[(2/s)^{1/2}(s/2-h_3^0)] + S[(2/s)^{1/2}(s/2+h_3^0)]\}).$$

The second integral in (3) is obtained by making a sign change on the variable h_3^0. When both are combined, we obtain

$$P(h_3^0)/2N_3^2 = s^{-3/2}2^{-1/2}\int_{h_3^0}[\{\cos[(\pi/s)(s/2+h_3^0)^2] - \cos[(\pi/s)(s/2-h_3^0)^2]\}\{C[(2/s)^{1/2}(s/2-h_3^0)] + C[(2/s)^{1/2}(s/2+h_3^0)]\} + \{\sin[(\pi/s)(s/2+h_3^0)^2] - \sin[(\pi/s)(s/2-h_3^0)^2]\} \times\{S[(2/s)^{1/2}(s/2-h_3^0)] + S[(2/s)^{1/2}(s/2+h_3^0)]\}]\,\mathrm{d}h_3^0. \quad (4)$$

To integrate over h_3^0, note that

$$\mathrm{d}\{C[(2/s)^{1/2}(s/2\mp h_3^0)]\}/\mathrm{d}h_3^0 = \mp(2/s)^{1/2}\cos[(\pi/s)(s/2\mp h_3^0)^2]$$

$$\mathrm{d}\{S[(2/s)^{1/2}(s/2\mp h_3^0)]\}/\mathrm{d}h_3^0 = \mp(2/s)^{1/2}\sin[(\pi/s)(s/2\mp h_3^0)^2].$$

This simplifies to

$$P(h_3^0) = (N_3^2/2s)(\{C[(2/s)^{1/2}(s/2-h_3^0)] + C[(2/s)^{1/2}(s/2+h_3^0)]\}^2 + \{S[(2/s)^{1/2}(s/2-h_3^0)] + S[(2/s)^{1/2}(s/2+h_3^0)]\}^2), \quad (5)$$

which is constructed from the pair of functions illustrated in Fig. 1. The Fresnel integrals $S(x)$ and $C(x)$ are readily evaluated using the following rational approximation (Abramowitz & Stegun, 1964)

$$C(X) = \tfrac{1}{2}+[(1+0{\cdot}926X)/(2+1{\cdot}792X + 3{\cdot}104X^2)]\sin(\pi/2)X^2 - [2+4{\cdot}142X+3{\cdot}492X^2 + 6{\cdot}670X^3]^{-1}\cos(\pi/2)X^2,$$

$$C(-X)=-C(X);$$

$$S(X) = \tfrac{1}{2}-[(1+0{\cdot}926X)/(2+1{\cdot}792X + 3{\cdot}104X^2)]\cos(\pi/2)X^2 - [2+4{\cdot}142X+3{\cdot}492X^2 + 6{\cdot}670X^3]^{-1}\sin(\pi/2)X^2,$$

$$S(-X)=-S(X).$$

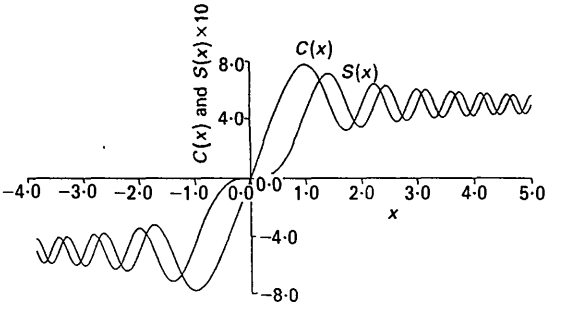

Fig. 1. Illustration of Fresnel cosine, $C(x)$, and sine, $S(x)$, functions for $\pm x$ spaces. Since $x=(s/2)^{1/2}\pm(2/s)^{1/2}h_3^0$, the + sign causes x to move from $(s/2)^{1/2}$ toward the $+x$ axis as h_3^0 increases from zero while the − sign causes x to move toward the $-x$ direction. Like pairs are added, squared and combined according to (5) to obtain $P(h_3^0)$.

In the case of a bent lamella, the parameter s is inversely proportional to R. As the bend radius goes to infinity, the X-ray broadening from the lamella should tend towards pure particle-size broadening $[P(h_3^0)/N_3^2 = \sin^2 \pi h_3^0/(\pi h_3^0)^2]$. Mathematically, we can illustrate this fact by taking the limit of (5) as $s \to 0$,

$$\lim_{s\to 0} P(h_3^0)/N_3^2$$
$$= \lim_{s\to 0} (1/2s)(\{C[(2/s)^{1/2}(s/2+h_3^0)]$$
$$+ C[(2/s)^{1/2}(s/2-h_3^0)]\}^2$$
$$+ \{S[(2/s)^{1/2}(s/2+h_3^0)]$$
$$+ S[(2/s)^{1/2}(s/2-h_3^0)]\}^2). \quad (6)$$

As $s \to 0$, the arguments of the Fresnel integrals in (6) tend towards infinity. For the argument $X > 5$, the sine and cosine Fresnel integrals can be approximated as (Abramowitz & Stegun, 1964)

$$\begin{matrix} C(X) \\ S(X) \end{matrix} = 0{\cdot}5 \pm (0{\cdot}3183099$$
$$- 0{\cdot}0968/X^4) \begin{matrix} \sin \\ \cos \end{matrix} \left(\frac{\pi}{2} X^2\right) \Big/ X$$
$$- (0{\cdot}10132 - 0{\cdot}154/X^4) \begin{matrix} \cos \\ \sin \end{matrix} \left(\frac{\pi}{2} X^2\right) \Big/ X^3$$
$$+ \varepsilon(X), \quad \varepsilon(X) < 3 \times 10^{-7}.$$

As $X \to \infty$, only the first two terms in the asymptotic expansion for $S(X)$ and $C(X)$ need be retained, since all other terms are negligible in comparison. Therefore, as $X \to \infty$,

$$\begin{matrix} C(X) \\ S(X) \end{matrix} = 0{\cdot}5 \pm 0{\cdot}3183099 \begin{matrix} \sin \\ \cos \end{matrix} \left(\frac{\pi}{2} X^2\right) \Big/ X. \quad (7)$$

Substituting (7) in (6), we get

$$\lim_{s\to 0} P(h_3^0)/N_3^2$$
$$= \lim_{s\to 0} [(0{\cdot}3183099)^2/4]$$
$$\times (\{\sin [(\pi/s)(h_3^0 + s/2)^2]/(h_3^0 + s/2)$$
$$- \sin [(\pi/s)(h_3^0 - s/2)^2]/(h_3^0 - s/2)\}^2$$
$$+ \{\cos [(\pi/s)(h_3^0 - s/2)^2]/(h_3^0 - s/2)$$
$$- \cos [(\pi/s)(h_3^0 + s/2)^2]/(h_3^0 + s/2)\}^2). \quad (8)$$

Expanding $(\pi/s)(h_3^0 \pm s/2)^2$ as $(\pi/s)\{[(h_3^0)^2 + s^2/4] \pm h_3^0 s\}$ and substituting appropriate trigonometric identities for $\sin(A \pm B)$, $\cos(A \pm B)$ in (8), one obtains

$$\lim_{s\to 0} P(h_3^0)/N_3^2$$
$$= \lim_{s\to 0} [(0{\cdot}3183099)^2/4]$$
$$\times \{[(2h_3^0\{\cos(\pi/s)[(h_3^0)^2 + s^2/4] \sin \pi h_3^0\}$$
$$- s\{\sin(\pi/s)[(h_3^0)^2 + s^2/4] \cos \pi h_3^0\})$$
$$\times [(h_3^0)^2 - s^2/4)]^{-1}]^2$$
$$+ [(2h_3^0\{\sin(\pi/s)[(h_3^0)^2 + s^2/4] \sin \pi h_3^0\}$$
$$+ s\{\cos(\pi/s)[(h_3^0)^2 + s^2/4] \cos \pi h_3^0\})$$
$$\times [(h_3^0)^2 - s^2/4]^{-1}]^2\}.$$

Simplifying and taking the limit as $s \to 0$, we find that

$$\lim_{s\to 0} P(h_3^0)/N_3^2 = \sin^2 \pi h_3^0/(\pi h_3^0)^2, \quad (9)$$

where the constant, 0·3183099, is identified as $1/\pi$. This well known result is illustrated in Fig. 2(a). The limit $s \to 0$ can be realized in two ways, either by letting $\Delta d/d \to 0$, or by letting $N_3 \to 0$.

For a second limit, the column height N_3 is made large.

$$\lim_{N_3\to\infty} P(h_3^0)/N_3^2$$
$$= \lim_{N_3\to\infty} [1/2N_3(\Delta d/\langle d\rangle)l]$$
$$\times [(C\{[2/N_3(\Delta d/\langle d\rangle)l]^{1/2}$$
$$\times [N_3 h_3 + N_3(\Delta d/\langle d\rangle)l/2]\}$$
$$+ C\{[2/N_3(\Delta d/\langle d\rangle)l]^{1/2}$$
$$\times [N_3(\Delta d/\langle d\rangle)l/2 - N_3 h_3]\})^2$$
$$+ (S\{[2/N_3(\Delta d/\langle d\rangle)l]^{1/2}$$
$$\times [N_3 h_3 + N_3(\Delta d/\langle d\rangle)l/2]\}$$
$$+ S\{[2/N_3(\Delta d/\langle d\rangle)l]^{1/2}$$
$$\times [N_3(\Delta d/\langle d\rangle)l/2 - N_3 h_3]\})^2].$$

The results of the calculation are as follows:

$$P(h_3)/N_3^2 = 1/N_3(\Delta d/\langle d\rangle)l, \quad |h_3| < 1 + (\Delta d/2\langle d\rangle)l$$
$$> 1 - (\Delta d/2\langle d\rangle)l$$
$$= 0, \quad |h_3| > 1 + (\Delta d/2\langle d\rangle)l$$
$$< 1 - (\Delta d/2\langle d\rangle)l, \quad (10)$$

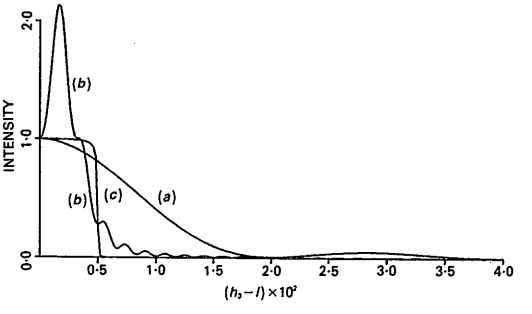

Fig. 2. Illustration of extreme and transitional X-ray diffraction line shapes from a bent crystal in h_3 space. Values of s are 0·5, 6, 5000, which correspond to N_3 values of (a) 50, (b) 500 and (c) 500 000. All are fixed at $\Delta d/\langle d\rangle = 0{\cdot}01$.

which describes the rectangular function illustrated in Fig. 2(*c*).

The Pearson VII (P VII) function provides an excellent description of instrumental broadening when a conventional diffractometer is used (Hall, Veeraraghaven, Ruben & Winchell, 1977; Naidu & Houska, 1982). Consequently, a measured curve is obtained by convoluting (5) with

$$Y = Y_0[1+(h_3-1)^2/ma^2]^{-m}, \qquad (11)$$

where

$$Y_0 = (\pi m)^{-1/2} a^{-1}\, \Gamma(m)/\Gamma(m-\tfrac{1}{2}).$$

Note that m alters the shape from a Cauchy ($m=1$) to a Gaussian ($m \geq 20$) and a largely determines the peak width. Both m and a are determined by least-squares fitting the P VII to the experimentally determined instrumental function (Naidu & Houska, 1982). Once these are known, one must carry out the convolution using a nine-point Gauss-Legendre quadrature, *i.e.*

$$P_m(h_3^0) = Y_0 \sum_{i=1}^{9} W_i[1+(bz_i)^2/ma^2]^{-m} P(h_3^0 - bz_i). \qquad (12)$$

This is carried out in h_3^0 space (Houska & Smith, 1981).

Discussion

Fig. 2 illustrates extreme variations of line shapes using a fixed $\Delta d/\langle d\rangle = 0{\cdot}01$ and $N_3 = 50$, 500 and 500 000. In the first case, the profile shape is almost pure particle-size broadening and, in the last case, it tends to the limit of a simple square shape or pure strain broadening as required by (10).

The transition from pure particle-size broadening to pure strain broadening occurs in a complicated way. An examination of the half-space plot of Fig. 2(*b*) illustrates a large positive oscillation about $h_3 = 0$. This example is based upon an s value that locates the peak origin at $x = 3^{1/2}$ in Fig. 1. However, a minimum in the intensity profile can be expected if the value of x with $h_3^0 = 0$ is near the first minimum of the Fresnel functions. When the Fresnel functions are introduced into (5) a small increase in $|h_3| > 0$ results in an increase in $P(h_3^0)$ until $x = 1{\cdot}15$ is reached. The latter locates a pair of symmetrical peaks with only one shown in the half space of Fig. 2. If the origin is relocated within the range $2{\cdot}12 \leq x \leq 2{\cdot}55$, we now find a peak at $h_3 = 0$ in addition to the symmetrical pair already described. From these examples, we can generalize and state that if $x(h_3^0 = 0)$ is located near a pair of maxima (Fig. 1), a peak will be found at $h_3 = 0$. Likewise, a minimum will be found at $h_3 = 0$ when x is located near a minimum and an even number of pronounced oscillations will be observed in the full h_3 space.

The maxima and minima of the intensity can be obtained more generally by taking the derivatives of (4) (or the integrand) and setting this equal to zero.

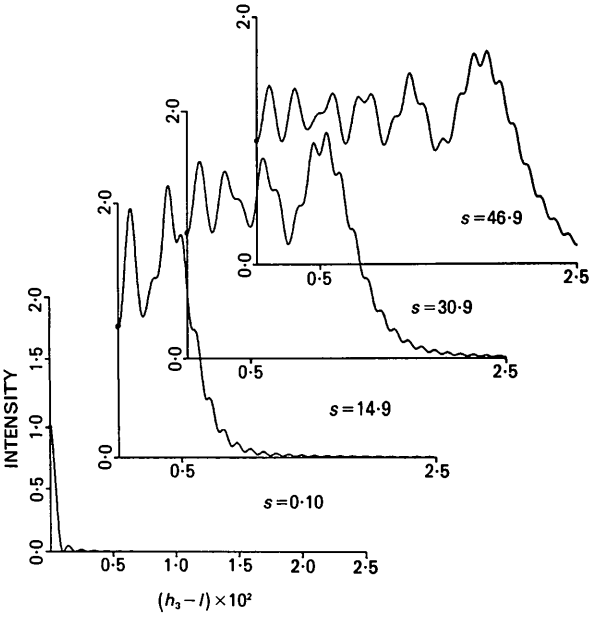

Fig. 3. Profile shapes in reciprocal space (h_3) for $s = 0{\cdot}10$, 14·9, 30·9 and 46·9, which correspond to $\Delta d/\langle d\rangle = 0{\cdot}0001$, 0·0149, 0·0309 and 0·0469. All are fixed at $N_3 = 1000$.

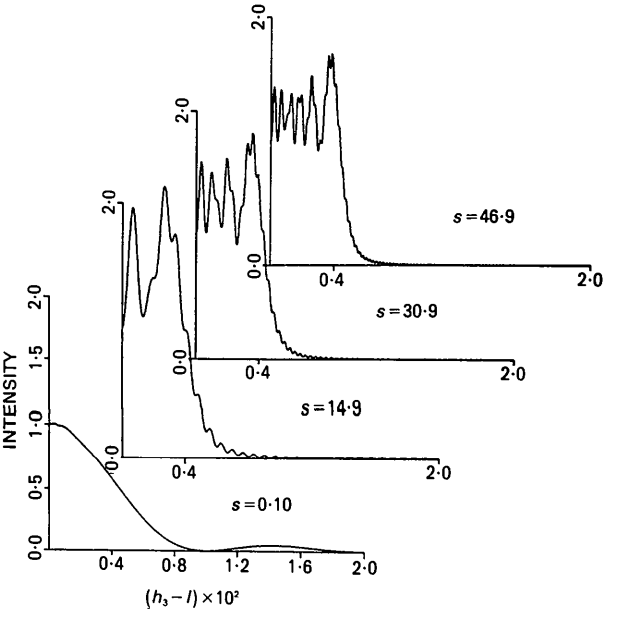

Fig. 4. Profile shapes in reciprocal space (h_3) for $s = 0{\cdot}10$, 14·9, 30·9 and 46·9, which correspond to $N_3 = 100$, 1490, 3090 and 4690. All are fixed at $\Delta d/\langle d\rangle = 0{\cdot}01$ except for $s = 0{\cdot}10$ where $\Delta d/\langle d\rangle = 0{\cdot}001$.

Table 1. *Ranges in s corresponding to the number of major oscillations*

s	Number of pronounced oscillations
0–5	1
5–9	2
9–13	3
⋮	⋮
4n−3–4n+1	n

After some simplifications, one obtains the following two solutions

$$\tan(\pi/s)[s^2/4+(h_3^0)^2] = \frac{S[(2/s)^{1/2}(s/2+h_3^0)]+S[(2/s)^{1/2}(s/2-h_3^0)]}{C[(2/s)^{1/2}(s/2+h_3^0)]+C[(2/s)^{1/2}(s/2-h_3^0)]}, \quad (13)$$

$$h_3^0 = \pm\text{integer}.$$

Figs. 3 and 4 give the profile shape *versus* h_3 for s values of 0·10, 14·9, 30·9 and 46·9 (all locate minimum positions in Fig. 1). In Fig. 3, s was increased by fixing N_3 at 1000 and increasing $\Delta d/\langle d\rangle$. The number of oscillations is seen to increase from 0 to 6, in steps of 2. Note that the width of the peak increases with increasing $\Delta d/\langle d\rangle$. As expected, the number of oscillations in the half space with $s \geq 14{\cdot}9$ is equal to the number of pairs of minima (sine, cosine) in the Fresnel functions between $x=0$ and $x=(s/2)^{1/2}$. In Fig. 4, s was increased by fixing $\Delta d/\langle d\rangle$ at 0·01 and increasing N_3. In this case, the width of the peak is a constant, whereas the number of oscillations increases.

It becomes evident from these results that approximate values of $\Delta d/\langle d\rangle$ and N_3 can be determined very simply. If $s>4$, then the ratio of the intensities at $h_3^0=\pm(s/2)[h_3=\pm\frac{1}{2}(\Delta d/\langle d\rangle)l]$ to that at $h_3^0=0(h_3=l)$ is approximately equal to one-fourth. Consequently, the width at one-fourth the intensity of the peak center can be used to estimate $\Delta d/\langle d\rangle$. Similarly, the number of pronounced oscillations in the full X-ray profile is given by int$[(s+3)/4]$ where int denotes 'integer part of'. From the preceding discussion, we have found that the peak width and the number of major oscillations can be used to estimate $\Delta d/\langle d\rangle$ and s. The latter being known N_3 can be calculated. Table 1 gives various ranges in s corresponding to the number of major oscillations. This procedure is only semi-quantitative and is suggested only for a quick interpretation of the intensity data. The most accurate determination of the parameters is obtained by least-squares fitting the experimental profile to (12). This may be carried out by beginning with estimates of $\Delta d/\langle d\rangle$ and N_3.

The authors are grateful to the National Science Foundation (Grant No. DMR-8000933) for funding this research.

References

ABRAMOWITZ, M. & STEGUN, I. (1964). *Handbook of Mathematical Functions.* Washington, DC: US Government Printing Office.
HALL, M. M., VEERARAGHAVEN, V. G., RUBEN, H. & WINCHELL, P. G. (1977). *J. Appl. Cryst.* **10**, 66–68.
HOUSKA, C. R. (1970). *J. Appl. Phys.* **41**, 69–75.
HOUSKA, C. R. (1978). *J. Appl. Phys.* **49**, 2991–2993.
HOUSKA, C. R. & SMITH, T. M. (1981). *J. Appl. Phys.* **52**, 748–754.
NAIDU, W. V. N. & HOUSKA, C. R. (1982). *J. Appl. Cryst.* **15**, 190–198.
WHITE, J. E. (1950). *J. Appl. Phys.* **21**, 855–859.
WILSON, A. J. C. (1949). *Acta Cryst.* **2**, 220–222.

Acta Cryst. (1985). A**41**, 517–528

The Calculation and Interpretation of Multiphonon X-ray Scattering – Example of Cubic Zincblende Structure Compounds

BY JOHN S. REID

Department of Natural Philosophy, The University, Aberdeen AB9 2UE, Scotland

(*Received* 18 *December* 1984; *accepted* 22 *March* 1985)

Abstract

The problems of making calculations using the total phonon scattering cross section in the harmonic approximation are examined and it is found that the method of Reid & Smith [*J. Phys. C* (1970), **3** 1513–1526] can be extended to cope with any material with a modest number of atoms per unit cell. Complex eigenvectors and complex scattering factors may be handled without approximations. The method is used to evaluate the multiphonon scattering (and one-phonon scattering) for a number of cubic zincblende structure compounds including GaAs, CdTe, CuI and SiC, taking eigendata from good lattice dynamical models. The results illustrate a discussion of the typical behaviour of multiphonon scattering as a

0108-7673/85/060517-12$01.50